Investigation on the Characteristics of the Envelope FDTD Based on the Alternating Direction Implicit Scheme

Saehoon Ju, *Student Member, IEEE*, Kyung-Young Jung, and Hyeongdong Kim, *Member, IEEE*

***Abstract*—This letter presents numerical characteristics of recently developed the envelope FDTD based on the alternating direction implicit scheme (envelope ADI-FDTD). Through numerical simulations, it is shown that the envelope ADI-FDTD is unconditionally stable and we can get better dispersion accuracy than the traditional ADI-FDTD by analyzing the envelope of the signal. This fact gives the opportunity to extend the temporal step size to the Nyquist limit in certain cases. Numerical results show that the envelope ADI-FDTD can be used as an efficient electromagnetic analysis tool especially in the single frequency or band limited systems.**

***Index Terms*—ADI technique, dispersion, envelope FDTD.**

I. Introduction

BECAUSE of the simplicity of programming and the capability of easy modeling for various electromagnetic materials and structures, the finite-difference time-domain (FDTD) method is so popular in the electromagnetics community [1]. In a FDTD calculation, the temporal step size must be smaller than or equal to the Courant-Friedrich-Levy (CFL) bound to guarantee the numerical stability. This condition restricts the applicability of the method especially in the case where the fine spatial grid relative to the wavelength is used to resolve fine geometrical features, since a fine spatial grid means the small temporal step size and an increase in computation time.

Recently, to overcome the limit of the CFL constraint, the alternating direction implicit algorithm (ADI) has been successfully applied to the FDTD method and leads to the unconditionally stable ADI-FDTD method [2]–[3]. It was reported that the ADI-FDTD has the potential to considerably reduce the number of time iterations used in the simulation. However, the ADI-FDTD is more efficient when the problem of interest requires high mesh resolution and/or high cell aspect-ratio [4], because its numerical accuracy decreases rapidly as the temporal step size increases. That is, although the temporal step size in ADI-FDTD is free from the stability constraint, we cannot extend the temporal step size to the Nyquist limit even in analyzing continuous wave (CW). This is because the temporal step size of ADI-FDTD is still bounded by the modeling accuracy. To improve the modeling accuracy of the conventional ADI-FDTD, the envelope ADI-FDTD has been developed by Rao *et al*. [5]. In the reference, the numerical results show that the envelope ADI-FDTD can be used as an efficient electromagnetic analysis tool.

In this letter, we present numerical stability and numerical dispersion through numerical test to demonstrate the characteristics of the envelope ADI-FDTD. The envelope ADI-FDTD modeling results for the two-dimensional (2-D) TM wave have been obtained to compare its numerical dispersion with those of traditional ADI-FDTD and FDTD. The purpose of this paper is to introduce the envelope ADI-FDTD formulation and discuss numerical stability and dispersion characteristic of the method.

II. Characteristics of the Envelope ADI-FDTD

Let us consider the governing equation for the envelope of electromagnetic quantities. Maxwell's curl equations for the envelope of electromagnetic fields in linear, isotropic, lossless, nondispersive media are given in the differential form by

$$\varepsilon\left(\frac{\partial \vec{E}}{\partial t}+j\omega_0\vec{E}\right)=\nabla\times\vec{H} \tag{1.a}$$

$$\mu\left(\frac{\partial \vec{H}}{\partial t}+j\omega_0\vec{H}\right)=-\nabla\times\vec{E}, \tag{1.b}$$

where ε, μ are the permittivity, permeability and ω_0 denotes the carrier frequency. $\vec{E}$ and $\vec{H}$ are the envelope signal of the electric field and the magnetic field, respectively. As in the ADI-FDTD [2]–[3], the envelope ADI-FDTD [5] also uses the ADI algorithm for time-marching scheme rather than the leap-frog algorithm of the conventional FDTD to circumvent the stability constraint. In the ADI algorithm, the envelope signals of all the field components are evaluated by two sub-iterations to get the one time step response. Due to the limited space, the equations for the envelope of x-directed electric field and magnetic field, E_x and H_x, are presented below.

- First iteration:

$$\varepsilon\left(\frac{\partial E_x}{\partial t}+j\omega_0 E_x\right)\Big|^{n+1/4}=\frac{\partial H_z}{\partial y}\Big|^{n+1/2}-\frac{\partial H_y}{\partial z}\Big|^{n} \tag{2a}$$

$$\mu\left(\frac{\partial H_x}{\partial t}+j\omega_0 H_x\right)\Big|^{n+1/4}=\frac{\partial E_y}{\partial z}\Big|^{n+1/2}-\frac{\partial E_z}{\partial y}\Big|^{n}. \tag{2b}$$

Manuscript received October 30, 2002; revised February 10, 2003. This work was supported by HY-SDR Center at Hanyang University, Seoul, Korea, under the ITRC program of MIC, Korea. The review of this letter was arranged by Associate Editor Dr. Rüdiger Vahldieck.

S. Ju is with the Microwave Engineering Laboratory, Department of Electrical and Computer Engineering, Hanyang University, Seoul 133-791, Korea.

K.-Y. Jung is with the Research and Development Laboratory, Curitel Communications, Inc., Seoul 137-070, Korea.

H. Kim is with the Department of Electrical and Computer Engineering, Hanyang University, Seoul 133-791, Korea (e-mail: hdkim@hanyang.ac.kr).

Digital Object Identifier 10.1109/LMWC.2003.815696

- Second iteration:

$$\varepsilon\left(\frac{\partial E_x}{\partial t}+j\omega_0 E_x\right)\Big|^{n+3/4}=\frac{\partial H_z}{\partial y}\Big|^{n+1/2}-\frac{\partial H_y}{\partial z}\Big|^{n+1} \tag{3a}$$

$$\mu\left(\frac{\partial H_x}{\partial t}+j\omega_0 H_x\right)\Big|^{n+3/4}=\frac{\partial E_y}{\partial z}\Big|^{n+1/2}-\frac{\partial E_z}{\partial y}\Big|^{n+1}. \tag{3b}$$

The superscript in (2) and (3) denotes a mapping point of the discrete time space. In the derivation of a set of implicit difference equations, it does not matter if we modify (2a) and (3a) of the envelope of electric fields or (2b) and (3b) of the envelope of magnetic fields. Here, following the procedure in by Zheng *et al.* [3], the *envelopes* of magnetic fields at $(n+1/2)$ time of the right-hand side in (2a) and (3a) are replaced by the corresponding magnetic field update equation at $(n+1/2)$ time. This leads following implicit equations for the envelope of E_x in each subiteration:

- First iteration at $(n+1/2)$ time:

$$\begin{aligned}&\left[1+\frac{2C_bD_b}{(\Delta y)^2}\right]E_x|^{n+1/2}_{i+1/2,j,k}-\frac{C_bD_b}{(\Delta y)^2}E_x|^{n+1/2}_{i+1/2,j+1,k}\\&-\frac{C_bD_b}{(\Delta y)^2}E_x|^{n+1/2}_{i+1/2,j-1,k}=C_a\,E_x|^{n}_{i+1/2,j,k}\\&+\frac{C_bD_a}{\Delta y}H_z|^{n}_{i+1/2,j+1/2,k}-\frac{C_bD_a}{\Delta y}H_z|^{n}_{i+1/2,j-1/2,k}\\&-\frac{C_b}{\Delta z}\left(H_y|^{n}_{i+1/2,j,k+1/2}-H_y|^{n}_{i+1/2,j,k-1/2}\right)\\&-\frac{C_bD_b}{\Delta y\Delta x}\left(E_y|^{n}_{i+1,j+1/2,k}-E_y|^{n}_{i,j+1/2,k}\right)\\&+\frac{C_bD_b}{\Delta y\Delta x}\left(E_y|^{n}_{i+1,j-1/2,k}-E_y|^{n}_{i,j-1/2,k}\right).\end{aligned} \tag{4}$$

- Second iteration at $(n+1)$ time:

$$\begin{aligned}&\left[1+\frac{2C_bD_b}{(\Delta z)^2}\right]E_x|^{n+1}_{i+1/2,j,k}-\frac{C_bD_b}{(\Delta z)^2}E_x|^{n+1}_{i+1/2,j,k+1}\\&-\frac{C_bD_b}{(\Delta z)^2}E_x|^{n+1}_{i+1/2,j,k-1}=C_a\,E_x|^{n+1/2}_{i+1/2,j,k}\\&-\frac{C_bD_a}{\Delta z}H_y|^{n+1/2}_{i+1/2,j,k+1/2}+\frac{C_bD_a}{\Delta z}H_y|^{n+1/2}_{i+1/2,j,k-1/2}\\&+\frac{C_b}{\Delta y}\left(H_z|^{n+1/2}_{i+1/2,j+1/2,k}-H_z|^{n+1/2}_{i+1/2,j-1/2,k}\right)\\&-\frac{C_bD_b}{\Delta z\Delta x}\left(E_z|^{n+1/2}_{i+1,j,k+1/2}-E_z|^{n+1/2}_{i,j,k+1/2}\right)\\&+\frac{C_bD_b}{\Delta z\Delta x}\left(E_z|^{n+1/2}_{i+1,j,k-1/2}-E_z|^{n+1/2}_{i,j,k-1/2}\right)\end{aligned} \tag{5}$$

where

$$C_a=\frac{(4\varepsilon-j\omega_0\varepsilon\Delta t)}{(4\varepsilon+j\omega_0\varepsilon\Delta t)},\quad C_b=\frac{(2\Delta t)}{(4\varepsilon+j\omega_0\varepsilon\Delta t)}$$

$$D_a=\frac{(4\mu-j\omega_0\mu\Delta t)}{(4\mu+j\omega_0\mu\Delta t)},\quad D_b=\frac{(2\Delta t)}{(4\mu+j\omega_0\mu\Delta t)}$$

and the integer i, j, k indicate that the corresponding basis function is located at $x=i\Delta x$, $y=j\Delta y$, $z=k\Delta z$ in the spatial grid. The envelope signals of electromagnetic field components are located on the same spatial grid as that of the tra-

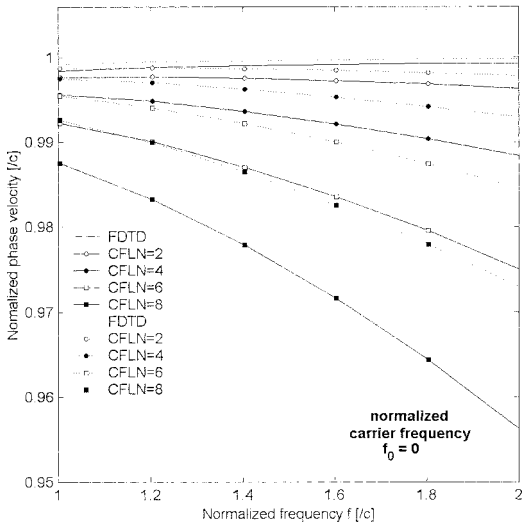

(a)

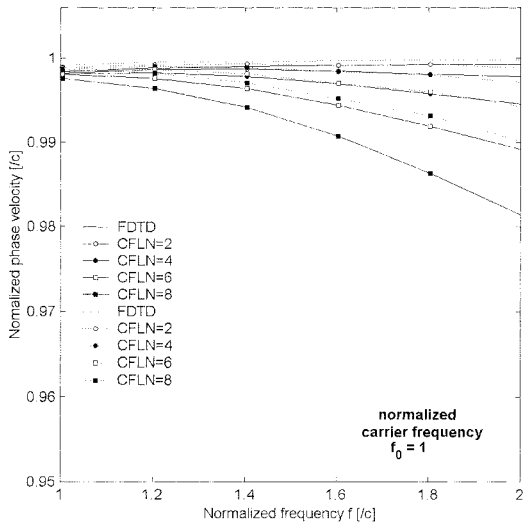

(b)

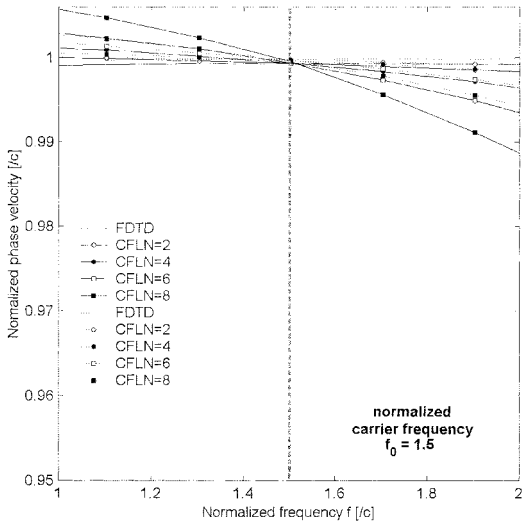

(c)

Fig. 1. Normalized numerical phase velocity of the envelope ADI-FDTD with different carrier frequencies (a) $\omega_0=0$, (b) $\omega_0=2\pi c$, and (c) $\omega_0=3\pi c$. The reference curve of the traditional FDTD is obtained with $\mathrm{CFLN}=1$. The wave-propagation angle of solid lines is 0° and that of dotted lines is 45°.

ditional FDTD. After updating the envlope signals of electric field components implicitly, those of magnetic fields components can be calculaed fully explicitly from the updated those of electric fields and previous values. Note that if the carrier frequency, ω_0, is zero, (2)–(5) are the same as those of the traditional ADI-FDTD [3].

The unconditional stability of the envelope ADI-FDTD can be demonstrated by a similar procedure described in [6]. In the envelope ADI-FDTD, the relationship for the n and $n+1$ time steps between the envelope of field components in the spectral domain can be summarized in a matrix form

$$X^{n+1} = \Lambda X^n \tag{6}$$

where the vector X denotes the envelope signals of six electromagnetic field components in the spectral domain, i.e., $X^{n+1} = \left[\vec{E}^{n+1} \quad \vec{H}^{n+1}\right]^T$ and $X^n = \left[\vec{E}^n \quad \vec{H}^n\right]^T$, where the superscript T denotes the matrix transpose. To verify the unconditional stability of the envelope ADI-FDTD independently of the carrier frequency ω_0, we have obtained eigenvalues of matrix Λ with various values of the carrier frequency ω_0 and the time step Δt. In this work, the eigenvalues of Λ was obtained numerically [7] because of the difficulty for getting the analytical solution. It was found that the absolute values of computed eigenvalues are equal to unity and the envelope ADI-FDTD is unconditionally stable. It should be mentioned that the selected values of carrier frequency ω_0 range between zero and $1/(2\Delta t)$, and the eigenvalues are less than unity if the material has a loss.

Next, we demonstrate the numerical dispersion characteristic of the envelope ADI-FDTD. For the sake of comparison with the results of the traditional ADI-FDTD and FDTD by Namiki and Ito [8], we simulated a line current source radiating in free-space for 2-D TM case. There are four observation points separated from the line current source. Two points are located in the axial direction (the wave-propagation angle is 0° or 90°) and the other points are placed in the diagonal direction (the wave-propagation angle is 45°). At the four observation points, to get the numerical phase velocity, the values of the electric fields are stored in time domain. Then we can calculate the numerical propagation constant, $\tilde{\beta}$, in the Fourier domain (or phasor domain) [1], [8]. Fig. 1 shows the normalized numerical phase velocity, $\tilde{v}_p = \omega/(\tilde{\beta}c)$, of the envelope ADI-FDTD with different carrier frequencies, i.e., $\omega_0 = 0$, $2\pi c$, $3\pi c$, where CFLN is defined as the ratio of the time step used in the simulation to the CFL stability limit of the traditional FDTD ($\mathrm{CFLN} = \Delta t/\Delta t_{CFL}$). Square grid is used for all the cases with $\Delta = \Delta x = \Delta y = \lambda/100$. Fig. 1(a) shows that numerical phase velocity of envelope ADI-FDTD is the same as that of the conventional ADI-FDTD [8] because the modulation frequency ω_0 is zero and then modeled quantity is not the envelope of the field but the field itself. The discrepancy between solid lines (the wave-propagation angle is 0° or 90°) and dot lines (the wave-propagation angle is 45°) denotes anisotropy of numerical waves in the computational lattice. In the envelope ADI-FDTD, the dispersion accuracy degrades rapidly around ω_0 as the time step increases. This comes from analyzing the slow-varying envelope of electromagnetic fields in the envelope ADI-FDTD. Therefore, we can make the numerical phase velocity comparable to the physical phase velocity even in higher frequency region by selecting the carrier frequency appropriately. In summary, the envelope ADI-FDTD improves numerical accuracy in higher frequency region by analyzing only the envelope of the fields. In the analysis of the electrically fine geometry, the envelope ADI-FDTD can be used efficiently because the simulation time step can be further increased while guaranteeing comparable numerical accuracy. Therefore, especially in getting sinusoidal steady state response or bandwidth limited response, the envelope ADI-FDTD can efficiently reduce the computational burden.

III. Conclusion

In this work, the numerical characteristics of the envelope ADI-FDTD are investigated. The envelope ADI-FDTD is unconditionally stable and can provide more accurate dispersion accuracy even in higher frequency region. The results imply that the method can be used as an efficient analysis method especially in the single frequency or band limited systems of electrically very fine geometry.

References

[1] A. Taflove and S. C. Hagness, *Computational Electrodynamics: The Finite-Difference Time-Domain Method*, 2nd ed. Norwood, MA: Artech House, 2000.

[2] T. Namiki, "A new FDTD algorithm based on alternating direction implicit method," *IEEE Trans. Microwave Theory Tech.*, vol. 47, pp. 2003–2007, Oct. 1999.

[3] F. Zheng, Z. Chen, and J. Zhang, "Toward the development of a three-dimensional unconditionally stable finite difference time-domain method," *IEEE Trans. Microwave Theory Tech.*, vol. 48, pp. 1550–1558, Sept. 2000.

[4] A. P. Zhao, "The influence of the time step on the numerical dispersion error of an unconditionally stable 3-D ADI-FDTD method: A simple and unified approach to determine the maximum allowable time step required numerical dispersion accuracy," *Microw. Opt. Tech. Lett.*, vol. 35, pp. 60–65, Oct. 2002.

[5] H. Rao, R. Scarmozzino, and R. M. Osgood Jr., "An improved ADI-FDTD method and its application to photonic simulations," *IEEE Photon. Technol. Lett.*, vol. 14, pp. 477–479, Apr. 2002.

[6] F. Zheng and Z. Chen, "Numerical dispersion analysis of the unconditionally stable 3-D ADI-FDTD method," *IEEE Microwave Theory Tech.*, vol. 49, pp. 1006–1009, May 2001.

[7] S. D. Gedney, G. Liu, J. A. Roden, and A. Zhu, "Perfectly matched layer media with CFS for an unconditionally stable ADI-FDTD method," *IEEE Trans. Microwave Theory Tech.*, vol. 49, pp. 1554–1559, Nov. 2001.

[8] T. Namiki and K. Ito, "Investigation of numerical errors of the two-dimensional ADI-FDTD method," *IEEE Trans. Microwave Theory Tech.*, vol. 48, pp. 1950–1956, Nov. 2000.